Bull. Natl. Mus. Nat. Sci., Ser. C, 46, pp. 1–14, December 25, 2020

Major and trace element analyses of igneous rocks and sediments by X-ray fluorescence spectrometry using glass bead and pressed powder pellet

Takashi Sano[1]*, Kenichiro Tani[1] and Arran P. Murch[1]

[1] Department of Geology and Paleontology, National Museum of Nature and Science, 4–1–1 Amakubo, Tsukuba, Ibaraki 305–0005, Japan
*Author for correspondence: sano@kahaku.go.jp

Abstract We report analytical methods to determine 10 major and 17 trace element contents in igneous rocks and sediments (that include ore and metamorphic rocks) using an X-ray fluorescence spectrometer (XRF). Two types of materials, glass beads and pressed powder pellets, were prepared for both igneous rock and sediment analyses. The glass beads of 38 igneous and 20 sediment standard samples were used to determine calibration curves (lines) of both igneous major elements (calibration type 1) and sediment major elements (calibration type 3). The pressed powder pellets of the standard samples were used to formulate calibration lines of both igneous trace elements (calibration type 2) and sediment trace elements (calibration type 4). We also applied the pressed powder pellets of sediment standard samples to make calibration lines for all the major and trace elements simultaneously (calibration type 5). Calibration types 1 to 5 were determined using an X-ray beam diameter of 30 mm. A further calibration line for all major and trace elements for sediment samples with an X-ray beam diameter of 10 mm was also determined (calibration type 6). Since sediment samples have larger variations of chemical compositions and inter-element effects (i.e., matrix effects) compared to igneous samples, matrix corrections were utilized for determining major elements of sediments (calibration types 3, 5 and 6). Peak overlap corrections for several trace elements (V, Cr, Co, As, Y, Zr, Nb, Ba) for both igneous and sediment samples were also conducted giving enhanced accuracy of the calibration lines (calibration types of 2, 4, 5, and 6). However, corrections were not applied to measurement of the igneous major elements (calibration type 1). Evaluations of the calibration lines for glass beads (calibration types 1 and 3) and replicate analyses for Geological Survey of Japan (GSJ) reference materials, JB-1, JR-1 and JSd-1, indicate an overall precision and accuracy on the order of 0.5% for Si, ca. 1% for Ti, Al, Fe, Mg, Ca, Na, K, P, and ca. 3% for Mn. The overall precision and accuracy of pressed powder pellets are on the order of 1–2% for Si, Ti, Al, Fe, Mn, Ca, Na, K, ca. 3–5% for Mn and Mg, and ca. 5–10% for the most trace elements. The new calibration lines were applied to determine the major and selected trace elements in three recently published GSJ reference materials (JB-1b, JA-1a and JSd-4).
Key words: XRF, igneous rock, sediment, whole rock analysis

Introduction

An X-ray fluorescence spectrometer (XRF) is a conventional and an effective tool to quantitatively analyze major and selective trace elements of igneous rocks and sediments. Compared to other methods such as wet chemical analyses and induced coupled plasma mass spectrometry (ICP-MS), it can rapidly analyze unknown samples with relatively high precision and reproducibility. However, since XRF analysis is a relative analysis, which uses calibration curves (lines) calculated from measuring the standard samples with reference values, the selection of standard samples, reliability of reference values, and consistency of analytical conditions are crucial to quantitatively analyze unknown samples.

It is evident that when a method of analysis gains popularity, to guarantee the quality of data produced, it is necessary to report the analytical method, and the accuracy and precision of analytical data in individual laboratories. We have already published several papers to report this data (Sano, 2002; Tani *et al.*, 2002, 2005; Sano *et al.*, 2011), however the analytical targets were restricted to igneous rocks. Since we have introduced a new XRF instrument (Rigaku ZSX Primus II) at the

National Museum of Nature and Science (NMNS), we expand our targets to sediments as well as ore and metamorphic rocks. This paper therefore reports (1) sample preparation procedures prior to the XRF analyses at NMNS, (2) analytical accuracy, precision, and detection limits for each element in igneous rocks and sediments (that include ore and metamorphic rocks), and (3) analytical results of relatively new Geological Survey of Japan (GSJ) reference materials (JB-1b, JA-1a and JSd-4) and the precision of them.

Sample preparations

Standard samples

As shown in Tables 1 and 2, we have selected 38 igneous rock and 20 sediment standard samples. Among the igneous rock standards, 18 samples are GSJ standard materials (JB-1a, JB-2, JB-3, JA-1, JA-2, JA-3, JR-2, JR-3, JG-1, JG-2, JG-3, JGb-1, JGb-2, JP-1, JF-1, JF-2, JH-1, JSy-1), 8 samples are United States Geological Survey (USGS) standard materials (RGM-1, BHVO-2, BIR-1a, DTS-2b, DNC-1, W-2a, AGV-2, GSP-2), and one sample is National Institute of Standards and Technology (NIST) standard material (Obsidian Rock 278). To cover a wide range of major and trace element contents in igneous rocks, 11 volcanic rocks from Iki Island in southwest Japan (Sano, 1995) were also selected (IK437, IK218, IK507, IK565, IK790, IK630, IK731, IK686, IK332, IK625, IK502). Among the sediment standards, 19 samples are GSJ standard materials that include ore and metamorphic rocks (JLk-1, JLs-1, JDo-1, JSl-1, JSl-2, JSd-1, JSd-2, JSd-3, JCh-1, JCp-1, JCt-1, JCFA-1, JMS-1, JMS-2, JSO-1, JMn-1, JCu-1, JZn-1, JH-1) and one sample is a standard material (JSS831-2) of the Japan Iron and Steel Federation (JISF). We note that the JH-1 (hornblendite) is selected for both the igneous and sediment standards. In addition, one synthetic material, SiO_2 (Cat. No. 37049-30, Kanto Chemical Co. Inc.), was also prepared to determine calibration curves (lines) of trace elements in the sediments.

Recommended values of the GSJ, USGS, NIST, and JISF standard materials are applied for the reference values in Tables 1 and 2 (Gladney and Roelandts, 1987, 1988; Gladney *et al.*, 1992; Terashima *et al.*, 1993, 1998; Imai *et al.*, 1995; GSL Geochemical Reference samples DataBase, AIST). When preferred values of the standard materials are reported by GeoRem, we adopt these values instead of the recommended values. For major element contents in Iki volcanic rocks, previous reference values used in the University of Tokyo determined by XRF are listed in Table 1 (Yoshida and Takahashi, 1997). The reference values of the selected trace elements in Iki volcanic rocks (Table 2) were precisely analyzed by ICP-MS at NMNS (Sano *et al.*, 2016). Major element contents in Table 1 were recalculated to 100% total with Fe as Fe_2O_3.

Preparation of sample powder

Sample powder conditions (e.g., grain size and homogeneity) are essential factors that influence the reproducibility of XRF analysis. Therefore, it is important to establish sample preparation procedures that can produce consistent well-conditioned sample powders minimizing variation. Since the standard materials of GSJ, USGS, NIST, and JISF are provided as powder samples, we used them for preparation of glass beads and pressed powder pellets (see below). Powder samples of Iki volcanic rocks were prepared using the following procedures. Unknown samples analyzed by XRF in NMNS were also prepared in the same way.

Prior to the sample crushing process, hand specimens of rock samples are cut into slabs (approximately $50 \times 50 \times 10$ mm in size) with a diamond-blade rock saw. This process is important to eliminate contamination from altered surfaces/veins, xenoliths, and xenocrysts. After checking for those contaminations the entire slab surface is polished with a resin-surfaced grinder with diamond grit to remove iron contamination from the rock saw. The polished slab is then rinsed with distilled water using an ultrasonic bath.

The sample slab is then coarsely crushed into grains with an alumina hammer (AL-143H, asOne Co., Ltd.) in an alumina pod (AL-143P, asOne Co., Ltd.). After crushing the grain size is usually 10 to 15 mm in diameter but will depend on the size of phenocrysts. For marine samples contamination of sodium chloride is removed at this stage (Tani *et al.*, 2005; Sano *et al.*, 2016).

The coarsely crushed sample is then washed

Table 1. Standard samples for major element analysis. The values are in wt%.

Igneous	SiO_2	TiO_2	Al_2O_3	Fe_2O_3[#]	MnO	MgO	CaO	Na_2O	K_2O	P_2O_5	Total
JB-1a	53.05	1.30	14.63	9.08	0.15	7.93	9.42	2.76	1.42	0.26	100.00
JB-2	52.85	1.18	14.54	14.32	0.22	4.59	9.75	2.03	0.42	0.10	100.00
JB-3	50.71	1.43	17.12	11.87	0.18	5.16	9.74	2.72	0.78	0.29	100.00
JA-1	64.44	0.86	15.33	7.07	0.16	1.58	5.74	3.87	0.78	0.17	100.00
JA-2	57.69	0.67	15.75	6.40	0.11	7.77	6.43	3.18	1.85	0.15	100.00
JA-3	62.37	0.70	15.59	6.53	0.10	3.73	6.25	3.20	1.41	0.12	100.00
JG-1	72.73	0.26	14.32	2.18	0.06	0.74	2.21	3.40	4.00	0.10	100.00
JG-2	77.27	0.04	12.54	0.97	0.06	0.04	0.70	3.56	4.74	0.08	100.00
JG-3	67.96	0.48	15.64	3.69	0.02	1.81	3.73	4.00	2.67	0.00	100.00
JGb-1	43.92	1.61	17.60	15.36	0.07	7.90	11.97	1.21	0.24	0.12	100.00
JP-1	43.68	0.01	0.68	8.90	0.12	45.96	0.57	0.02	0.00	0.06	100.00
JF-1	67.26	0.00	18.23	0.08	0.00	0.01	0.94	3.40	10.07	0.01	100.00
JF-2	65.75	0.01	18.65	0.06	0.00	0.00	0.09	2.41	13.03	0.00	100.00
278	73.20	0.25	14.18	2.04	0.05	0.23	0.99	4.85	4.17	0.04	100.00
JR-2	76.51	0.11	13.01	0.90	0.10	0.12	0.68	4.08	4.47	0.02	100.00
JR-3	73.67	0.21	12.05	4.74	0.08	0.05	0.09	4.75	4.34	0.02	100.00
RGM-1	74.09	0.27	13.83	1.88	0.04	0.28	1.16	4.11	4.34	0.00	100.00
IK437	48.25	2.73	17.03	10.98	0.18	5.96	8.02	3.64	2.45	0.76	100.00
IK218	46.82	2.78	16.12	10.76	0.17	7.99	9.26	4.32	1.04	0.74	100.00
IK507	48.72	2.50	16.97	10.61	0.15	6.92	8.75	2.57	2.23	0.58	100.00
IK565	48.79	2.25	16.82	11.58	0.17	5.77	9.84	3.35	1.12	0.31	100.00
IK790	51.00	1.81	17.05	10.42	0.14	6.02	7.52	3.98	1.61	0.45	100.00
IK630	54.33	2.18	18.17	9.45	0.12	2.44	4.82	4.20	3.70	0.59	100.00
IK731	54.81	1.61	17.79	7.59	0.17	3.07	5.52	5.01	3.77	0.66	100.00
IK686	60.78	1.52	16.39	6.11	0.08	2.74	4.26	3.83	3.88	0.41	100.00
IK332	64.75	0.70	18.60	3.73	0.04	0.17	1.68	5.03	5.11	0.19	100.00
IK625	77.16	0.10	13.31	1.16	0.01	0.00	0.30	3.14	4.79	0.03	100.00
IK502	76.89	0.08	12.98	0.98	0.03	0.00	0.37	4.03	4.61	0.03	100.00
BHVO-2	49.79	2.72	13.47	12.27	0.17	7.21	11.37	2.21	0.52	0.27	100.00
BIR-1a	47.60	0.95	15.38	11.21	0.17	9.63	13.20	1.81	0.03	0.02	100.00
DTS-2b	40.56	0.00	0.46	7.99	0.00	50.85	0.12	0.02	0.00	0.00	100.00
DNC-1	47.20	0.48	18.36	9.98	0.15	10.14	11.50	1.89	0.23	0.07	100.00
W-2a	52.81	1.06	15.49	10.86	0.17	6.39	10.89	2.21	0.00	0.14	100.00
AGV-2	60.21	1.07	17.17	6.79	0.00	1.82	5.28	4.25	2.92	0.49	100.00
GSP-2	67.57	0.67	15.12	4.97	0.00	0.97	2.13	2.82	5.46	0.29	100.00
JGb-2	47.13	0.57	23.81	6.78	0.13	6.27	14.30	0.93	0.06	0.02	100.00
JH-1	49.13	0.68	5.77	10.47	0.19	17.06	15.32	0.72	0.54	0.10	100.00
JSy-1	60.55	0.00	23.38	0.08	0.00	0.02	0.25	10.84	4.86	0.01	100.00
Sediment	SiO_2	TiO_2	Al_2O_3	Fe_2O_3[#]	MnO	MgO	CaO	Na_2O	K_2O	P_2O_5	Total
JLk-1	64.78	0.76	18.96	7.85	0.30	1.97	0.78	1.19	3.18	0.24	100.00
JLs-1	0.21	0.00	0.04	0.03	0.00	1.08	98.57	0.00	0.01	0.05	100.00
JDo-1	0.41	0.00	0.03	0.04	0.01	35.02	64.39	0.02	0.00	0.07	100.00
JSl-1	63.44	0.77	18.77	7.22	0.06	2.57	1.58	2.33	3.03	0.22	100.00
JSl-2	63.32	0.80	19.35	7.08	0.09	2.54	2.01	1.43	3.20	0.17	100.00
JSd-1	68.70	0.66	15.12	5.22	0.10	1.87	3.13	2.82	2.25	0.13	100.00
JSd-2	61.57	0.62	12.47	11.80	0.12	2.77	3.71	2.47	1.16	0.11	[##]96.79
JSd-3	79.98	0.42	10.43	4.60	0.16	1.23	0.59	0.43	2.07	0.09	100.00
JCh-1	98.46	0.03	0.74	0.36	0.02	0.08	0.05	0.03	0.22	0.02	100.00
JCp-1	0.00	0.00	0.17	0.01	0.00	0.30	98.40	1.08	0.04	0.00	100.00
JCt-1	0.00	0.00	0.09	0.00	0.00	0.09	98.71	1.08	0.02	0.00	100.00
JCFA-1	52.39	1.36	25.13	5.39	0.07	2.20	9.23	2.32	1.32	0.61	100.00
JMS-1	60.55	0.79	17.82	7.77	0.11	3.23	2.40	4.59	2.52	0.20	100.00
JMS-2	47.34	1.59	16.07	12.42	2.56	3.67	5.30	6.56	3.06	1.43	100.00
JSO-1	50.81	1.63	23.88	15.25	0.27	2.80	3.40	0.88	0.45	0.64	100.00
JMn-1	17.72	1.33	5.40	18.08	41.55	3.92	3.65	3.52	1.18	0.68	[##]97.02
JCu-1*	34.53	0.01	0.36	28.89	0.66	2.68	28.29	0.06	0.02	0.00	[##]95.51
JZn-1	47.45	0.22	6.86	18.31	1.63	2.23	19.54	0.49	0.89	0.00	[##]97.60
JH-1	49.13	0.68	5.77	10.47	0.19	17.06	15.32	0.72	0.54	0.10	100.00
JSS831-2**	4.03	7.34	3.63	79.03	0.63	3.38	1.43	0.11	0.07	0.34	100.00

* A glass bead of JCu-1 (to formulate calibration line 3) is not present.
** A pressed lellet of JSS831-2 (to formulate calibration lines 5 and 6) is not present.
[#] Total iron as Fe_2O_3.
[##] Totals are not 100% because $>$1 wt% of Ni, Cu and/or Zn are present in these samples.

Table 2. Standard samples for trace element analysis. The values are in ppm.

Igneous	S	V	Cr	Co	Ni	Cu	Zn	Rb	Sr	Y	Zr	Nb	Ba	Ce	Pb	Th
JB-1a	10.2	205	392	38.6	139	56.7	82.1	39.2	442	24	144	26.9	504	65.9	6.76	9.03
JB-2	17.9	575	28.1	38	16.6	225	108	7.37	178	24.9	51.2	1.58	222	6.76	5.36	0.35
JB-3	9.86	372	58.1	34.3	36.2	194	100	15.1	403	26.9	97.8	2.47	245	21.5	5.58	1.27
JA-1	21.6	105	7.83	12.3	3.49	43.0	90.9	12.3	263	30.6	88.3	1.85	311	13.3	6.55	0.8
JA-2	8.0	126	436	29.5	130	29.7	64.7	72.9	248	18.3	116	9.47	321	32.7	19.2	5.03
JA-3	214	169	66.2	21.1	32.2	43.4	67.7	36.7	287	21.2	118	3.41	323	22.8	7.7	3.25
JG-1	10.9	25.2	53.2		7.47	2.52	41.1	182	184	30.6	111	12.4	466	45.8	25.4	13.2
JG-2	7.0	3.78	6.37	3.62	4.35	0.49	13.6	301	17.9	—	118	14.7	—	48.3	31.5	31.6
JG-3	54.7	70.1	22.4	11.7	14.3	6.81	46.5	67.3	—	17.3	—	5.88	—		11.7	8.28
JGb-1	1910	635	57.8	60.1	25.4	85.7	109	6.87	—	10.4	—	3.34	—	8.17	1.92	0.48
JP-1	26.9	27.6	2807	116	2460	6.72	41.8	0.8	3.32	1.54	5.92	1.48	64.3	0.19	0.12	0.19
JF-1	—	5.43	5.48	0.12	1.36	0.82	4.41	266	172	2.84	38.6	0.74	1750	4.19	33.4	1.17
JF-2	2.8	4.86	2.47	0.68	1.38	0.78	1.4	218	200	2.67	6.73	0.7	298	0.84	48.7	0.31
278	—	—	6.1	1.5	3.6	5.9	55	127.5	63.5	—	—	—	—	62.2	16.4	12.4
JR-2	9.6	3	3.1	0.46	1.99	1.36	27.8	303	8.11	—	96.3	18.7	39.5	38.8	21.5	31.4
JR-3	39	4.2	3.5	0.98	1.6	2.9	209	453	10.4	166	1494	510	65.8	327	32.8	112
RGM-1	—	13	3.7	2	—	12	32	150	110	25	220	8.9	810	47	24	15
IK437	—	168	—	31.7	64.4	22.1	28.8	49.8	644	29.3	279	47.6	585	77.0	4.5	5.0
IK218	—	213	—	39.8	137.6	35.6	2.6	105.0	684	27.5	255	54.0	574	77.0	3.6	5.1
IK507	—	235	—	36.3	77.8	32.8	120.2	59.1	606	35.0	243	50.5	917	85.4	1.6	2.2
IK565	—	303	—	37.7	29.5	39.7	100.6	24.3	913	37.1	136	20.8	414	42.9	3.5	2.2
IK790	—	168	—	37.4	76.3	27.1	87.0	37.5	463	85.3	213	29.9	397	56.6	4.6	4.2
IK630	—	125	—	17.5	3.3	13.4	77.7	67.4	551	53.0	339	52.6	729	94.8	5.2	7.3
IK731	—	66	—	15.4	28.3	16.6	23.9	99.4	631	25.2	339	81.8	696	103.0	6.3	13.3
IK686	—	104	—	18.7	54.9	16.2	66.4	109.3	377	30.0	210	45.0	659	74.9	10.1	11.4
IK332	—	7	—	2.8	0.1	2.7	70.6	113.4	282	34.0	465	69.2	1112	87.8	9.1	12.4
IK625	—	4	—	0.87	0.6	1.8	26.0	273.7	5	24.6	98	73.3	8	39.9	16.0	50.8
IK502	—	2	—	1.22	0.2	1.6	19.1	376.1	2	38.4	100	94.0	4	47.2	20.1	47.2
BHVO-2	168	317	280	45	119	127	103	9.8	389	26	172	18	130	38	—	1.2
BIR-1a	70	310	370	52	170	125	70	—	110	16	18	0.6	6	2	3	—
DTS-2b	—	22	15500	120	3780	3	45	2	—	—	—	—	16	—	4	—
DNC-1	—	148	270	57	247	100	70	4.5	144	18	38	3	118	—	6.3	—
W-2a	79	260	92	43	70	110	80	21	190	23	100	7.9	170	23	9.3	2.4
AGV-2	—	120	17	16	19	53	86	68.6	658	20	230	15	1140	68	13	6.1
GSP-2	—	52	20	7.3	17	43	120	245	240	28	550	27	1340	410	42	105
JGb-2	599	174	125	25.8	13.6	11.4	209	2.9	438	4.5	11.6	1.9	36.5	3	1.5	0.19
JH-1	567	228	616	51.5	58.2	8.6	48.5	14.4	153	13.7	48.3	4.2	106	17.6	2.6	1.4
JSy-1	13	2.1	2	0.16	1.1	1.3	61.8	66.3	19.3	2.6	70.2	0.51	15.7	2.6	4.9	0.23

Sediment	S	V	Cr	Co	Ni	Cu	Zn	As	Rb	Sr	Y	Zr	Nb	Ba	Ce	Pb	Th
JLk-1	1052	117	69	18	35	62.9	152	26.8	147	67.5	40	137	15.8	574	87.9	43.7	19.5
JLs-1	123	3.59	3.37	0.083	0.362	0.268	3.19	0.145	0.18	295	0.223	4.19	1		0.521	0.7	0.029
JDo-1	90.5	3.14	7.93	0.168	2.9	1.41	35.4	0.114	1.75	116	10.3	6.21	0.4	6.14	2.49	0.95	0.043
JSl-1	1467	131	60.9	15.5	37.6	40.8	108	14.9	117	193	30	174	9.53	305	60.6	17.4	9.97
JSl-2	579	122	64.7	15.7	40.6	44.5	101	11.4	118	230	31.3	191	12.3	302	69.6	19.7	11.5
JSd-1	68	76	21.5	11.2	7.04	22	96.5	2.42	67.4	340	14.8	132	11.1	520	34.4	12.9	4.44
JSd-2	13100	125	108	48.4	92.8	1117	2056	38.6	26.9	202	17.4	111	4.56	1199	23.4	146	2.33
JSd-3	399	70.4	35.3	12.7	19.6	426	136	252	285	58.7	14.9	124	7.8	462		82.1	
JCh-1	4	10.4	7.04	15.5	8.76	15.3	7.93	0.567	8.61	4.2	1.81	11.5	1.7	302	5.21	2	0.735
JCp-1	1920	—	—	—	—	—	0.5	—	—	7240	—	—	—	10.3	—	—	—
JCt-1	192	—	—	—	—	—	0.5	—	—	1410	—	—	—	6.1	—	—	—
JCFA-1	1960	—	75	37.4	32.2	122	—	29.1	54.1		—	—	—	—	—	47.2	—
JMS-1	—	127	133	18.1	53	88	264	18	88	154	24.3	132	—	307	—	49	—
JMS-2	—	183	78	226	311	447	166	35	65	454	254	220	—	1856	—	—	—
JSO-1	—	300	71	32	39	169	105	8.1	14.5	196	24.9	96	—	267	—	13	—
JMn-1	940	424	26.6	1732	12632	11132	1068	—	10.9		—	—	27.6	—	277	—	—
JCu-1	—	9	10	324	425	37300	690	—	1.9	75	—	—	—	3.5	—	4	—
JZn-1	—	24	21	24	6	29	22200	99	—	358	—	—	—	208	—	1610	—
JH-1	567	—	616	51.5	58.2	8.6	61.8		14.4	153	13.7	48.3	4.2	106	17.6	2.6	1.4
SiO2	0	0	0	0	0	0	0	0	0	0	0	—	0	0	0	0	0

ultrasonically twice in a high-grade acetone or ethanol (10 min) and twice in de-ionized Milli-Q water (10 min). The rinsed sample grains are then dried in an oven at 110°C for at least 12 hours.

The dried sample is then put into the alumina pod for further crushing using the alumina hammer. Samples are crushed into $<$1 mm sized grains. To keep the homogeneity of the sample, all the fine material generated by crushing is collected and used in the mill grinding.

Finally, the finely crushed sample is grinded in a mill, Multi-beads Shocker (Yasui Kikai Co. Ltd.). The sample and a cylindrical alumina rod are put into a polycarbonate vessel (50 cm^3 in volume) and grinded at a rotary speed of 3000 rpm. Generally, grinding of 60–90 seconds is enough to obtain a fine

powder. We note that prior to the main grinding, 0.5 to 1 g of the sample grains are pre-grinded to avoid contamination from earlier samples. After grinding the sample, the cylindrical alumina rods are cleaned by grinding quartz sand (Cat. No. 172-00015, FUJIFILM Wako Pure Chemical Industries Ltd.).

Preparation of glass bead

The fused glass bead technique is commonly used to measure major elements in XRF analysis (e.g., Kimura and Yamada, 1996; Yamasaki, 2014). This technique has the advantage of reducing inter-element effects (matrix effects), improving homogeneity of the analyzed samples, and eliminating sample particle size effects.

Loss on ignition (LOI) values are determined prior to major element analysis by weighing 0.5–1 g of powder on an analytical balance system (Shimazu AUX120) before and after heating the powder at 900–1025℃ for 4 hours in an electric muffle furnace. To make the fused glass bead, lithium tetraborate ($Li_2B_4O_7$, Cat. No. 120-04455, FUJIFILM Wako Pure Chemical Industries Ltd.) is used as a flux. After the flux is dried at 110℃ for more than 12 hours, 4.0000 ± 0.0002 g of flux and 0.4000 ± 0.0002 g of the sample powder dried in the muffle furnace are weighed directly in a 95% platinum and 5% gold alloy crucible (type CS-2; 32 mm in diameter) to minimize error in weighing. Then the flux and sample powder are mixed on a vibration tough-mixer. Before fusing, two drops (~0.1 g) of lithium iodine aqueous solution ($LiI : H_2O = 0.4 : 10$ in weight) are added as an exfoliation agent. After putting a platinum lid on the crucible, fusion and agitation is automatically carried out with a high frequency bead sampler (TK-4200A, Tokyo Kagaku Co. Ltd.). Fusing conditions are 280 seconds for fusion and 180 seconds for agitation, both at 1100 ℃.

Preparation of pressed powder pellet

The pressed powder pellet technique is used to analyze major and selected trace elements. The advantage of using pressed powder pellets is its high sensitivity, ideal for trace element analyses. However, careful corrections are required for spectral line overlaps for trace elements and matrix effects for major elements as described below. The powder pellet technique also has an advantage in analyzing trace elements that are concentrated in refractory minerals (e.g., Zr in zircon and Cr in chromspinel). The fused glass bead method in XRF and acid digestion method in ICP-MS often have difficulty completely dissolving these minerals.

Before the preparation of the pressed powder pellet, sample powder was dried in an oven at 110℃ for at least 12 hours. Sample powder for determination of all major and trace element contents (calibration type 5 and 6 as explained below) was further heated at 900–1025℃ for 4 hours in an electric muffle furnace. Since all volatiles (mainly H_2O) are evaporated by the heating, the total weight of major element contents should become 100 wt%.

The sample powder (~4–5 g) is put into a polyvinyl chloride (PVC) ring (inner diameter of 31 mm and outer diameter of 38 mm; Cat. No. 3399J301, Rigaku Co. Ltd.) and pressed under iron molds at 150 kN. This pressure is kept for 60 seconds, and then slowly released to obtain a smooth surfaced sample pellet. If the amount of sample powder is a small (＜1 g), a PVC ring with a small diameter (inner diameter of 13 mm and outer diameter of 18 mm; Cat. No. 5200-540-02351, PANalytical Div., Spectris Co. Ltd.) is used to make the pellet using a pressure of ~2 kN. The advantage of using PVC rings is that a binding material to solidify the pellet is not required thus avoiding contamination from the binder. However, small particles of the powder float during analysis of pressed powder pellets and contaminate the measuring chamber. To avoid contamination, the pressed powder pellet is covered by 2.5 micron-thick film (Mylar polyester film: Cat. No. 100, Chemplex Industries Inc.) during the XRF analysis.

Analytical methods

Instrument and analytical conditions

XRF analysis was carried out using a Rigaku ZSX Primus II at the Division of Mineral Science, Department of Geology and Paleontology, NMNS. A Rh anode X-ray tube was fitted in the spectrometer. The accelerating voltage and tube current were set at 50 kV and 50 mA, respectively.

The analytical elements were Si, Ti, Al, Fe, Mn, Mg, Ca, Na, K and P for major elements, and S, V,

Table 3. Analytical conditions.

Material	Element	X-ray	Slit	Crystal	Detector	Angle (2θ)			Counting time (s)				PHA	Interfere element (line)
						peak	$^{\$}$B.G. (low)	B.G (high)	peak	B.G.	peak	B.G.		
bead	Si	Kα	S4	PET	PC	109.1			20				100–300	
bead	Ti	Kα	S2	LiF(200)	SC	86.1	84.8	88.0	40	20			100–320	
bead	Al	Kα	S4	PET	PC	144.7			20				100–300	
bead	Fe	Kα	S2	LiF(200)	SC	57.5			20				100–350	
bead	Mn	Kα	S2	LiF(200)	SC	63.0	62.0	64.0	40	20			100–330	
bead	Mg	Kα	S4	RX25	PC	38.3	36.5	40.0	40	20			100–300	
bead	Ca	Kα	S4	LiF(200)	PC	113.1			20				100–300	
bead	Na	Kα	S4	RX25	PC	46.6	44.0	49.0	40	20			100–300	
bead	K	Kα	S4	LiF(200)	PC	137.0	134.0	139.0	40	20			100–300	
bead	P	Kα	S4	Ge	PC	141.1	139.0	143.0	40	20			100–300	
									D = 3 cm		D = 1 cm			
pellet	Si*	Kα	S4	PET	PC	109.1	107.0	111.0	10	5	20	10	100–300	
pellet	Ti	Kα	S2	LiF(200)	SC	86.2	84.8	88.0	10	5	20	10	100–320	
pellet	Al*	Kα	S4	PET	PC	144.7	141.0	147.0	10	5	20	10	100–300	
pellet	Fe*	Kα	S2	LiF(200)	SC	57.5	56.5	58.5	10	5	20	10	100–350	
pellet	Mn	Kα	S2	LiF(200)	SC	63.0	62.0	64.0	10	5	20	10	100–330	
pellet	Mg	Kα	S4	RX25	PC	38.3	36.5	40.0	10	5	20	10	100–300	
pellet	Ca*	Kα	S4	LiF(200)	PC	113.1	111.0	115.0	10	5	20	10	100–300	
pellet	Na	Kα	S4	RX25	PC	46.6	45.0	48.0	10	5	20	10	100–300	
pellet	K	Kα	S4	LiF(200)	PC	137.0	134.0	139.0	10	5	20	10	100–300	
pellet	P	Kα	S4	Ge	PC	141.1	139.0	143.0	10	5	20	10	100–300	
									D = 3 cm		D = 1 cm			
pellet	V	Kα	S2	LiF(200)	SC	77.0	76.0	78.0	40	20	40	20	100–300	Ti (Kβ)
pellet	Cr	Kα	S2	LiF(200)	SC	69.3	68.5	70.2	40	20	40	20	100–300	V (Kβ)$^{\#\#}$
pellet	Co	Kα	S2	LiF(200)	SC	52.8	50.5	54.0	40	20	40	20	100–310	Fe (Kβ)
pellet	Ni	Kα	S2	LiF(200)	SC	48.6	48.0	49.3	40	20	40	20	100–300	
pellet	Cu	Kα	S2	LiF(200)	SC	45.0	44.5	45.5	40	20	40	20	100–300	
pellet	Zn	Kα	S2	LiF(200)	SC	41.8	41.0	42.5	40	20	40	20	100–300	
pellet	As**	Kα	S2	LiF(200)	SC	34.0	33.5	34.5	200	100			100–300	Pb (Lα)
pellet	Rb	Kα	S2	LiF(200)	SC	26.6	25.7	27.8	40	20	40	20	100–300	
pellet	Sr	Kα	S2	LiF(200)	SC	25.1	24.5	25.7	40	20	40	20	100–300	
pellet	Y	Kα	S2	LiF(200)	SC	23.8	23.2	24.5	40	20	40	20	100–300	Rb (Kβ)
pellet	Zr	Kα	S2	LiF(200)	SC	22.5	21.8	23.1	40	20	40	20	100–300	Sr (Kβ)
pellet	Nb	Kα	S2	LiF(200)	SC	21.3	20.9	21.7	80	40	120	60	100–300	Y (Kβ)
pellet	Ba	Lα	S2	LiF(200)	SC	87.2	84.5	88.5	80	40	200	100	100–300	Ti (Kα)
pellet	Ce$^{\#}$	Lβ1	S2	LiF(200)	SC	71.6	71.0	72.5	120	60			100–300	Zr (Kα2)
pellet	Pb$^{\#}$	Lβ1	S2	LiF(200)	SC	28.2	27.8	28.7	80	40			100–280	
pellet	Th	Lα	S2	LiF(200)	SC	27.4	27.1	27.8	80	40	200	100	100–300	
pellet	S	Kα	S4	Ge	PC	110.8	109.0	113.0	40	20	120	60	150–280	

* attenuator is 1/10 when diamter is 3 cm.
** only available for sediment measurement.
$^{\#}$ not available when diameter is 1 cm.
$^{\#\#}$ The interfere correction is not conducted for igneous rocks (calibration line 2).
$^{\$}$ B.G.: background.

Cr, Co, Ni, Cu, Zn, As, Rb, Sr, Y, Zr, Nb, Ba, Ce, Pb and Th for trace elements (Table 3). The most suitable slit (S2 or S4), crystal (PET, RX25, Ge or LiF) and detector (proportional counter, PC or scintillation counter, SC) were selected for each element analysis (Table 3). An automated wavelength-range scan program of the ZSX Primus II was used to determine the wavelength positions of peaks and the backgrounds of analyzed spectra as well as setting up the energy path range of the pulse height analyzer. The Kα line was measured for all major elements and most trace elements, but the Lα line was measured for Ba and the Lβ1 line for Ce and Pb measurements. I_p/I_b (net over background intensity, or S/N) ratios of Si, Al, Fe and Ca were adequately high for igneous samples, and therefore, X-ray intensities at peak positions were used for net intensities (i.e., no background correction was conducted). In contrast, background intensities cannot be ignored for other elements to get accurate calibration lines. Likewise, I_p/I_b ratios of the four major elements (Si, Al, Fe, Ca) in some sediment samples are low. Therefore, X-ray intensities at both lower and higher angles against a peak position were used for background corrections for all elements except for the four major elements (Si, Al, Fe, Ca) in the igneous samples (Table 3). Adequate counting time for peak and background of each element was set based on intensity of the element measurement. In order to improve precision in the determination,

three measurements were conducted for trace element analyses.

Types of calibration lines

In order to get accurate element contents in whole rock samples, we adopt the calibration line method for the XRF analysis. X-ray intensities of the peak and background are both affected by X-ray absorption, enhancement, sample material, sample particle size, and geometry effects. Since material and geometry of igneous rocks are different from those of sediments, calibration lines of igneous rocks are generally different than those of sediments. We have therefore prepared multiple (six) types of calibration lines as follows (Table 4).

Table 4. Types of calibration lines adopted at National Museum of Nature and Science.

Material (Diameter)	Glass bead (30 mm)	Pressed pellet (30 mm)	Pressed pellet (10 mm)
Igneous rock (Major elements)	1		
Igneous rock (Trace elements)		2	
Sediment (Major elements)	3		
Sediment (Trace elements)		4	
Sediment (All elements with drying)		5	6

Note: Names of calibration lines in ZSX Prius II program: 1. ig-mj-3 cm, 2. ig-tr-3 cm, 3. sd-mj, 4. sd-tr-3 cm, 5. sd-dry-all-3 cm, 6. sd-dry-all-1 cm, Measurement time: 1. 11 minutes, 2. 90 minutes, 3. 13 minutes, 4. 110 minutes, 5. 120 minutes, 6. 125 minutes

Type 1: Major elements in igneous rocks with an X-ray beam diameter of 30 mm. To make the calibration lines, glass beads of 38 igneous standard materials were used (Table 1).

Type 2: Trace elements in igneous rocks with an X-ray beam diameter of 30 mm. To make the calibration lines, pressed powder pellets of 38 igneous standard materials were used (Table 2).

Type 3: Major elements in sediments that include ore and metamorphic rocks with an X-ray beam diameter of 30 mm. To make the calibration lines, glass beads of 19 sediment standard materials were used (Table 1).

Type 4: Trace elements in sediments with an X-ray beam diameter of 30 mm. To make the calibration lines, pressed powder pellets of 20 sediment standard materials were used (Table 2).

Type 5: Major and trace elements in sediments with an X-ray beam diameter of 30 mm. To make the calibration lines, pressed powder pellets of 20 sediment standard materials were used (Table 2).

Type 6: Major and trace elements in sediments with

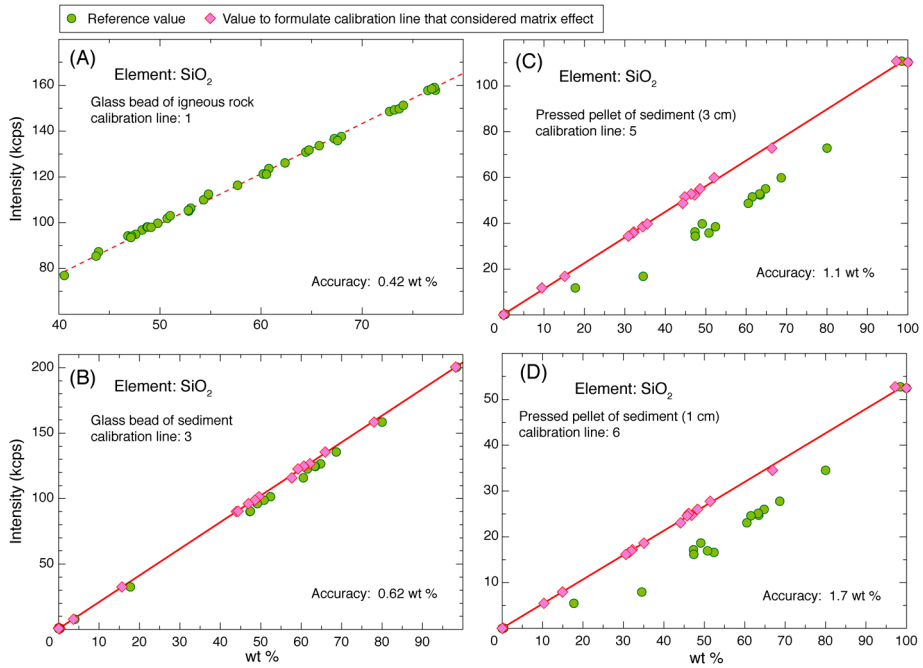

Fig. 1. Calibration lines for SiO_2. X-ray intensities before and after matrix correction are plotted against the content of each element. Red solid lines show the calibration lines after matrix correction. Red dotted lines show calibration lines before correction. Values of accuracy for calibration line are from Table 5.

an X-ray beam diameter of 10 mm. To make the calibration lines, pressed powder pellets of 20 sediment standard materials were used (Table 2).

All the calibration lines are calculated using software equipped with ZSX Primus II, and linear functions were adopted for all elements (Fig. 1). We therefore call the calibration curves calibration lines in this paper. Measurement times of all elements per one sample for each calibration type is shown in Table 4.

Setting up of calibration lines

Major elements

In XRF analysis, it is necessary to correct the net count rate of X-rays from the standard samples for inter-element effects (matrix effects), so as to convert X-ray intensity to content (e.g., Czamanske *et al.*, 1966). The matrix effect increases with increasing element contents, and can thus be reduced by dilution. However, even with a dilution factor of 10 (that adopted here), the X-ray fluorescent intensity of an element is affected by enhancement or suppression from coexisting matrices (e.g., Yamsaki, 2014 and references there in).

In spite of the matrix effects, Fig. 1A and Table 5 show the accuracy of the calibration lines without the matrix correction for calibration type 1 (major elements of igneous rocks) is the same as that reported using other instruments (e.g., Yamasaki, 2014). This indicates that the matrix effects are negligibly small for the compositional ranges of the igneous rocks in this study (Table 5).

In contrast, matrix corrections are needed for calibration types 3, 5 and 6 (major elements in sediment samples) as shown in Fig. 1B–D. We therefore determined the matrix factors by measuring the 19 (for glass bead) and 20 (for pressed powder pellets) sediment standard samples. A software equipped in the instrument was used and an adsorption correction model was adopted for the determinations. Table 6 shows that there are slight differences observed among the matrix correction factors for calibration types 3, 5, and 6. Generally, glass beads (calibration type 3) gave smaller errors than pressed powder pellets (calibration types 5 and 6). However, obvious differences between the matrix correction factors of 30 mm pellets (calibration type 5) and 10 mm pellets (calibration type 6) cannot be identified. The matrix correction was calculated using the following equation:

$$W_{i,cor} = W_i(1 + \Sigma A_{ij} W_j) \quad (1)$$

where $W_{i,cor}$, W_i, A_{ij}, and W_j are content of element i after the correction, content of element i before the correction, the matrix correction factor, and content of element j, respectively. Fig. 1B–D shows that accurate calibration lines were made with the matrix corrections.

Trace elements

I_p/I_b ratios are more important for trace element measurements. Therefore, X-ray intensities at both lower and higher angles against a peak position were used for background corrections for all trace elements (Table 3), as denoted above.

For trace element analysis, peak overlaps from coexisting elements are another problem. Fig. 2A, C shows an example of VKα interfered by TiKβ and Fig. 2B, D shows another example of YKα interfered by RbKβ. The problem of peak overlaps is obvious when we see the relationship between X-ray intensity and Y content of IK502 in Fig. 2B. IK502 contains high Y and Rb (Table 2). Without an overlap correction, the YKα calibration line (red dotted line in Fig. 2B) is drawn off from the reference value (38.4 ppm) of IK502, leading to an overestimation of the content (77.4 ppm; see an interaction between black arrow and red dotted line in Fig. 2B). Fig. 2B shows the intensity (i.e., I_p–I_b) of YKα is increased by the addition of Rb. To reduce the effect of the interfering element (e.g., Rb) we use an overlap coefficient. To determine the overlap coefficient, we used certain amounts (e.g., reference values) of an interfering element by using a software equipped in the instrument. The peak overlap is corrected by the following equation:

$$W_{i,cor} = W_i + B_{ij} W_j \quad (2)$$

where $W_{i,cor}$, W_i, B_{ij}, and W_j are content of element i after the correction, content of element i before the correction, the overlap coefficient, and content of element j, respectively. The overlap of TiKβ line to VKα line, VKβ line to CrKα line, FeKβ line to CoKα line, PbLα line to AsKα line, RbKα line to YKα line, SrKβ line to ZrKα line, YKβ line to

Table 5. Range of standard sample composition and accuracy of correlation curves (lines).

	Igneous (#calib. lines 1 & 2)			Sediment (#calib. lines 3 & 4)			Sediment (#calib. line 5)			Sediment (#calib. line 6)		
	lower limit	upper limt	##Accuracy	lower limit	upper limt	##Accuracy	lower limit	upper limt	##Accuracy	lower limit	upper limt	##Accuracy
SiO_2 (wt%)	40.56	77.27	0.42	0	98.46	0.62	0	98.46	1.1	0	98.46	1.7
TiO_2	0	2.78	0.022	0	7.34	0.0084	0	1.63	0.0071	0	1.63	0.011
Al_2O_3	0.46	23.81	0.2	0.03	25.13	0.18	0.03	25.13	0.2	0.03	25.13	0.28
Fe_2O_3*	0.06	15.36	0.2	0	79	0.097	0	18.76	0.16	0	18.76	0.23
MnO	0	0.22	0.0068	0	42.8	0.0062	0	42.82	0.002	0	42.82	0.045
MgO	0	50.85	0.25	0.08	35.02	0.067	0.08	35.02	1.2	0.08	35.02	1.1
CaO	0.09	15.32	0.1	0.05	98.71	0.097	0.05	98.71	0.97	0.05	98.71	1.8
Na_2O	0.02	10.84	0.077	0	6.56	0.043	0	6.56	0.057	0	6.56	0.12
K_2O	0	13.03	0.064	0	3.20	0.049	0	3.20	0.029	0	3.20	0.042
P_2O_5	0	0.76	0.009	0	1.43	0.017	0	1.43	0.085	0	1.43	0.068
S (ppm)**	0	1910	31	0 1900	1900 13100	200 3000	—	—	—	—	—	—
V	0	635	13	0	424	14	0	424	14	0	424	14
Cr**	0 125 436	125 436 15500	7 10 170	0	616	11	0	616	13	0	616	15
Co**	0	120	5.7	0 100	100 1732	11 79	0 100	100 1732	7.6 68	0 100	100 1732	8.9 72
Ni**	0 120	120 3780	7.1 18	0 80	80 12632	7.2 110	0 80	80 12632	7.1 130	0 50	50 12632	7.6 110
Cu**	0	225	6.1	0 400	400 37300	5.7 1500	0 400	400 37300	6.8 1500	0 400	400 37300	6.9 1500
Zn**	0	209	14	0 250	250 22200	16 420	0 250	250 22200	19 440	0 250	250 22200	19 450
As	—	—	—	0	173	3.1	—	—	—	—	—	—
Rb**	0 60	60 453	1.6 22	0 50	50 285	3.8 5	0 50	50 285	3.2 5	0 50	50 285	3.1 4.6
Sr**	0	913	37	0 200	200 7240	20 97	0 200	200 7240	20 73	0 200	200 7240	21 80
Y**	0 50	50 166	2.7 9.5	0	254	4.8	0	254	4	0	254	4
Zr	0	1494	25	0	344	19	0	220	20	0	220	17
Nb**	0 12 50	12 50 510	1.9 4.3 12	0	27.6	1.4	0	27.6	1.3	0	27.6	1.5
Ba**	0	1750	28	0 1200	1200 1856	36 $	0 1200	1200 1856	30 $	0 1200	1200 1856	30 $
Ce**	0 100	100 420	7.9 1.7	0	277	3.8	0	277	5.4	—	—	—
Pb**	0 10	10 48.7	1 1.2	0 120	120 1610	3.1 $	0 120	120 1610	3.6 $	—	—	—
Th**	0 10 50	10 50 112	0.49 1.8 8.1	0	19.5	0.36	0	19.5	0.48	0	19.5	1.1

* Total iron as Fe_2O_3.

** For several trace elements, calibration lines are separated by two or three depend on their concentrations (low, high and/or middle).

Type of calibration line (see Table 4).

Accuracy of calibration line is calculated by a equation = $\{\Sigma(C_{mes} - C_{rec})^2/(n-2)\}^{1/2}$, where C_{mes} is measured value, C_{rec} is recommended (or certified) value, and n is number of samples.

$ Accuracy is not reported because a calibration line of the concentration range was formulated by using 2 samples, indicating that standard deviation was not calculated.

Table 6. Matrix correction factors.

Element	SiO_2	TiO_2	Al_2O_3	Fe_2O_3*	MnO	MgO	CaO	Na_2O	K_2O	P_2O_5	Cu
**Calibration line 3 (sediment glass bead 30 mm)											
SiO_2	—	0.004557	0.000592	0.000847	0.001980	−0.000314	0.002059	0.002671	0.005018	0.001196	—
TiO_2	−0.021168	—	−0.023005	−0.022120	−0.023096	−0.022827	−0.029208	−0.031275	−0.028423	−0.005991	—
Al_2O_3	−0.000290	−0.011043	—	0.002146	0.001998	0.001127	0.000576	0.006895	0.001802	0.000749	—
Fe_2O_3	−0.001821	0.001416	−0.002111	—	0.002617	−0.003664	0.005142	−0.005157	0.010030	0.023157	—
MnO	−0.002252	0.045325	−0.008734	−0.007224	—	−0.007587	0.004915	−0.037558	0.016610	0.130996	—
MgO	−0.001560	−0.052343	0.001850	0.005286	0.000419	—	−0.000547	0.005357	0.009753	−0.015196	—
CaO	−0.000542	−0.012759	0.002269	0.000514	−0.000376	0.000204	—	0.023383	0.012975	−0.107275	—
Na_2O	−0.004736	0.009648	−0.003364	−0.004989	−0.001947	−0.004178	0.001732	—	0.014610	−0.037707	—
K_2O	−0.012307	0.008452	−0.012843	−0.015436	−0.012179	−0.011692	−0.011172	−0.011022	—	−0.008864	—
P_2O_5	−0.012412	−0.031568	−0.010469	−0.009784	−0.013028	−0.012519	−0.011094	−0.013451	−0.003087	—	—
Calibration line 5 (sediment pressed pellet 30 mm)											
SiO_2	—	0.278794	0.002449	0.009754	0.004793	−0.007700	0.014128	0.004345	0.012264	−0.187655	0.000016
TiO_2	−0.005020	—	−0.005289	−0.005955	−0.006228	−0.009443	0.010703	−0.000640	0.017058	−0.030024	—
Al_2O_3	−0.006509	−0.003298	—	−0.001990	0.003728	−0.001727	0.011229	0.007320	0.027998	0.024698	—
Fe_2O_3	−0.005993	0.027123	−0.007641	—	−0.003146	−0.009170	0.005324	−0.002028	0.009166	−0.028986	—
MnO	0.023196	0.344435	−0.004972	0.022151	—	−0.016859	0.109361	−0.007532	0.119914	0.068587	—
MgO	—	—	—	—	—	—	—	—	—	—	—
CaO	0.008602	−0.549639	0.007234	−0.005283	0.004774	−0.002097	—	0.016583	−0.258261	0.078908	—
Na_2O	−0.010670	0.071043	−0.013546	−0.016433	−0.012150	−0.009332	−0.011987	—	−0.009908	−0.065543	—
K_2O	−0.016011	0.112974	−0.024618	−0.019490	−0.017715	−0.017781	−0.013096	−0.016596	—	−0.106406	—
P_2O_5	−0.008092	−0.025594	−0.003893	−0.014177	−0.005574	−0.007186	−0.008448	−0.078805	−0.002181	—	—
Calibration line 6 (sediment pressed pellet 10 mm)											
SiO_2	—	0.116549	0.014177	0.002283	0.005379	−0.005144	0.020299	0.002535	−0.011222	−0.045460	0.000018
TiO_2	−0.004979	—	−0.004853	−0.003724	−0.006604	−0.010798	0.013730	0.004017	0.020696	−0.067022	—
Al_2O_3	−0.007843	−0.080226	—	−0.008896	−0.000124	−0.003617	0.004079	−0.000322	0.002086	0.066170	—
Fe_2O_3	−0.005914	0.020192	−0.007248	—	−0.002881	−0.008819	0.005708	−0.002195	0.009663	−0.022395	—
MnO	−0.003009	0.177889	−0.013307	−0.001193	—	−0.012152	0.015372	−0.010800	0.040080	−0.093258	—
MgO	—	—	—	—	—	—	—	—	—	—	—
CaO	0.013346	−0.770217	0.009742	−0.010511	0.009469	−0.002549	—	0.023459	−0.359644	1.084820	—
Na_2O	−0.012289	0.103681	−0.019220	−0.018840	−0.016457	−0.009364	−0.016558	—	−0.019139	−0.116522	—
K_2O	−0.016217	0.100570	−0.024581	−0.019759	−0.017746	−0.017457	−0.0137425	−0.015487	—	−0.100750	—
P_2O_5	−0.000928	−0.003889	−0.003966	−0.014284	−0.007110	−0.007655	−0.009423	−0.008230	−0.006593	—	—

* Total iron as Fe_2O_3.
** Type of calibration line (see Table 4)

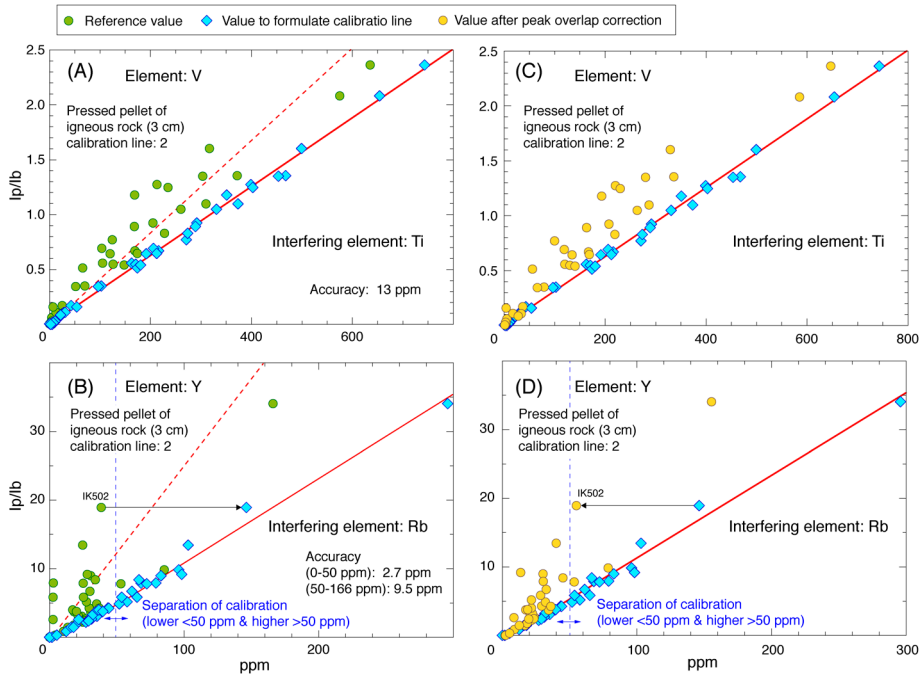

Fig. 2. (A) (B) Calibration lines for V and Y. X-ray intensities before and after peak overlap correction are plotted against the content of each element. Red solid lines show the calibration lines after peak overlap correction. Red dotted lines show calibration lines before correction. In (B), plots of IK502 sample are connected with thin black arrow. (C) (D) Value to formulate calibration line and value after peak overlap correction for V and Y. Since Y values to formulate calibration line include effect of Rb interference, the effect is deducted to get accurate Y value (e.g., see black arrow connecting values of IK502 sample in (D)). Values of accuracy for calibration line are from Table 5.

NbKα line, TiKα line to BaLα line, and ZrKα2 line to CeLβ1 line were corrected (Table 3). Fig. 2 shows two examples of the peak overlap correction. Although intensities of the standard materials decrease at the same contents, values of accuracy for calibration lines with peak overlap corrections are distinctly better than those without corrections (Fig. 2A, B). Since the horizontal axis of the accurate calibration lines include effects of an interfering element (e.g., Rb in Fig. 2B), the effect should be deducted to get exact element contents (Fig. 2C, D). For example, Y content of IK502 (55.0 ppm; yellow circle in Fig. 2D) following correction became closer to the reference value (38.4 ppm). The calibration lines for several trace elements are separated into low, (middle), and high concentration regions to increase the correlation efficiencies (Fig. 2B, D; Table 6).

Results and Discussion

Analytical precision, accuracy and detection limit

To check analytical precision and accuracy, three GSJ standard samples (JB-1, JR-1 and JSd-1) were analyzed 10 times each (Table 7). We note that JB-1 and JR-1 were not used to formulate the calibration lines (Tables 1, 2). For an X-ray beam diameter of 30 mm (calibration types 1–5) the values of precision, indicated as 1σ of standard deviations, of major elements are less than 0.05 wt%, particularly for elements with a lower content such as TiO_2, Fe_2O_3, MnO, CaO, CaO, K_2O and P_2O_5, all of which were less than 0.01 wt%. For the trace elements, the values of precision are less than 2 ppm except for S (up to 13.7 ppm), Cr (up to 2.7 ppm), Sr (up to 2.6 ppm), Ba (up to 4.4 ppm) and Ce (up to 3.3 ppm). The values of precision for calibration type 6 (the beam diameter of 10 mm) are distinctly (~2 times) larger than those for other calibration lines (Table 7). This is due to lower X-ray intensities (~1/10) for calibration type 6 compared with those of other calibration types.

As explained above, errors for type 1 calibration lines (igneous major elements with glass beads) are similar to those reported using other instruments (e.g., Yamasaki, 2014). Likewise, errors for type 2 calibration lines (igneous trace elements with pressed powder pellets) are similar to those of our previous reports (e.g., Tani *et al.*, 2005; Sano *et al.*, 2011). These facts suggest that analytical methods adopted here give accurate and precise results for igneous rock measurements. On the other hand, errors for type 3 calibration lines (sediment major elements with glass bead) and type 4 calibration lines (sediment trace elements with pressed powder pellets) are generally higher than those of types 1 and 2 calibration lines (Table 5), caused by large matrix effects in sediment samples. Similar to the precision, the errors for the type 6 calibration line (the beam diameter of 10 mm) are larger than those for other calibration lines (the beam diameter of 30 mm), due to the low X-ray intensities.

The errors for calibration lines, which is the inverse of accuracy of calibration lines, are sufficiently larger than those of precision for all elements, therefore errors of the accuracy are considered as uncertainties in the XRF analysis (e.g., Tani *et al.* 2005; Sano *et al.*, 2011). The average values of JB-1, JR-1 and JSd-1 in this study are within the accuracy for the preferred (and/or recommended) values for almost of all samples and elements (Table 7). Therefore, accurate determinations have been conducted by the methods of this study. However, the average values are different from the preferred (and/or recommended), even if we consider 2σ errors of the accuracy for three cases; Pb in JB-1 (6.1 ppm vs. 10 ppm), Nb in JR-1 (26.1 ppm vs. 15.2 ppm), and JSd-1 (7.8–7.9 ppm vs. 11.1 ppm). We therefore pay careful attention to the Pb content in basalts and Nb content in silicic rocks in our analytical data.

The accuracy of calibration lines (Table 5), and the precision and analytical values of JB-1, JR-1 and JSd-1 (Table 7) show an overall precision and accuracy on the order of 0.5% for Si, ca. 1% for Ti, Al, Fe, Mg, Ca, Na, K, P, and ca. 3% for Mn. The overall precision and accuracy of pressed powder pellets, as shown in Tables 5 and 7, is on the order of 1–2% for Si, Ti, Al, Fe, Mn, Ca, Na, K, ca. 3–5% for Mn and Mg, and ca. 5–10% for the most trace elements.

To check pulse height analyzer (PHA) fluctuation, a PHA reference sample (Rigaku Co Ltd.) is analyzed before every series of measurements. If the peak position of the pulse height (200 ± 20) and/or the peak resolution (PC < 40%, SC < 60%) of the

Table 7. Reproducibility of GSJ standard samples. Note that the standard samples (except for JSd-1) were not used to formulate the calibration lines (see Tables 3 and 4).

	JB-1			JB-1b			JA-1a			JR-1			JSd-4			JSd-1						
	average	S.D.[##]	recom.[$]	average	S.D.	recom.	average	S.D.	recom.	average	S.D.	recom.	average	S.D.	recom.	average	S.D.	average	S.D.	average	S.D.	recom.
Calib. line[*]	1 & 2			1 & 2			1 & 2			1 & 2			3 & 4			3 & 4		5		6		
SiO_2 (wt %)	52.49	0.046	52.37	51.57	0.042	51.11	63.63	0.035	63.66	75.3	0.091	75.45	52.37	0.058	51.12	67.55	0.041	66.63	0.430	66.98	0.574	66.55
TiO_2	1.33	0.004	1.32	1.24	0.003	1.26	0.90	0.003	0.87	0.11	0.001	0.11	0.69	0.003	0.64	0.64	0.002	0.63	0.004	0.62	0.004	0.643
Al_2O_3	14.43	0.013	14.53	14.26	0.023	14.38	15.8	0.022	15.4	13.06	0.022	12.83	13.61	0.017	13.22	14.78	0.019	14.61	0.158	14.72	0.079	14.65
Fe_2O_3[**]	8.96	0.007	8.99	8.89	0.007	9.02	7.35	0.005	7.17	0.80	＜0.001	0.89	8.40	0.005	8.06	5.01	0.004	4.91	0.043	4.84	0.043	5.059
MnO	0.15	0.001	0.153	0.15	0.001	0.147	0.16	0.001	0.157	0.10	＜0.001	0.099	0.12	0.001	0.107	0.09	＜0.001	0.09	0.001	0.09	0.001	0.0924
MgO	7.82	0.018	7.71	8.52	0.015	8.14	1.63	0.008	1.55	0.20	0.007	0.12	4.11	0.011	4.04	1.75	0.007	2.4	0.037	2.39	0.051	1.813
CaO	9.32	0.006	9.25	9.55	0.007	9.6	5.8	0.005	5.74	0.73	＜0.001	0.67	5.64	0.007	5.57	3.1	0.003	2.78	0.021	2.79	0.080	3.034
Na_2O	2.81	0.017	2.77	2.64	0.017	2.63	3.98	0.02	3.9	3.93	0.025	4.02	2.25	0.016	2.28	2.71	0.012	2.48	0.335	2.82	0.096	2.727
K_2O	1.46	0.002	1.43	1.3	0.002	1.32	0.78	0.001	0.78	4.56	0.004	4.41	1.54	0.007	1.4	2.26	0.009	2.14	0.057	2.18	0.031	2.183
P_2O_5	0.26	0.001	0.255	0.25	0.001	0.256	0.16	0.001	0.165	0.03	0.001	0.021	0.50	0.003	0.45	0.14	0.001	0.15	0.005	0.15	0.026	0.122
LOI[#]	0.98	0.06	1.30	1.88	0.11	2.02	0.26	0.03	n.r.[¥¥]	1.62	0.16	1.31	11.14	0.19	n.r.	2.62	0.09	2.62	0.09	2.62	0.09	
Total	100.01		100.08	100.25		99.88	100.19			100.44		99.93	100.37			100.65		99.44		100.20		
S (ppm)	55	13.7	19.4	0	12.6	n.r.	0	1.4	n.r.	0	2.0	13.3	[$$]31104	925.2	n.r.	73	4.7	n.d.		n.d.		68
V	203	2.0	211	212	2.1	214	117	1.2	107	8	0.9	7	130	1.3	157	83	0.8	78	1.0	76	1.8	76
Cr	436	2.7	425	368	1.6	439	5	0.7	4.1	1	0.7	2.8	[$$]1515	11.1	1220	15	1	14	1.4	12	4.2	21.5
Co	40	0.7	38.2	37	0.4	40.3	21	0.2	12.8	0	0.3	0.8	31	0.5	21	16	0.1	18	1.5	18	6.1	11.2
Ni	141	0.9	133	156	0.6	148	0	0.5	1.8	5	0.6	1.7	128	1.5	118	9	0.3	10	0.7	11	1.7	7.04
Cu	63	1.4	55.1	60	1.3	55.5	55	3.4	41.8	5	0.6	2.7	1074	13.1	488	23	0.4	23	0.2	24	1.9	22
Zn	84	0.4	85.2	74	0.4	80	90	0.4	90.7	43	0.3	30.6	2362	7.3	1480	102	0.6	102	0.8	102	2.1	96.5
As	n.d.[¥]		2.33	n.d.		1.24	n.d.		n.r.	n.d.		16.3	66	0.2	n.r.	3	0.1	n.d.		n.d.		2.42
Rb	39.6	0.2	41.3	34.9	0.3	39.1	12.8	0.3	n.r.	269.9	0.7	257.0	49.8	2.3	57	75.5	0.3	75	0.3	75	1.1	67.4
Sr	420	0.7	444	417	0.9	439	282	0.5	267	31	0.2	29.1	240	1.1	223	483	2.6	465	2.3	465	4.3	340
Y	20.6	0.2	24.3	20.6	0.3	n.r.	35	0.3	31.7	52.7	0.2	45.1	18.7	0.9	21	11.2	0.3	11.5	0.3	11.5	1.1	14.8
Zr	134	0.3	141	128	0.3	n.r.	95	0.2	94.9	105	0.4	99.9	122	0.6	90	144	1.1	175	0.7	164	1.9	132
Nb	29.9	0.2	33.3	22.5	0.2	n.r.	6.3	0.1	n.r.	26.1	0.2	15.2	6.9	0.1	n.r.	7.8	0.1	7.9	0.1	7.8	0.3	11.1
Ba	496	4.3	493	505	4.0	n.r.	320	4.8	321	68	2	50.3	851	7.5	892	493	4.4	481	2.8	482	10.7	520
Pb	6.1	0.3	10	4.9	0.3	6.8	6	0.5	n.r.	20	0.5	19.3	368	1.4	240	13.5	0.4	12.7	0.4	n.d.		12.9
Ce	53.9	1.5	67.8	56.7	2.5	n.r.	15.7	2.1	n.r.	48.8	2.3	47.2	50.1	2.9	n.r.	32.2	3.3	32.2	3.3	n.d.		34.4
Th	8.1	0.3	9.3	8.5	0.4	n.r.	1	0.3	n.r.	26.9	0.2	26.7	8.3	0.5	n.r.	4.4	0.6	4.2	0.5	4.8	0.9	4.44

[*] Type of calibratio line (see Table 4).
[**] Total iron as Fe_2O_3.
[#] LOI of recommended value is calculated by $LOI = H_2O - FeO[(55.85*2 + 16*3)/\{(55.85 + 16)*2\} - 1]$.
[##] S.D.: One sigma standard deviation of the replicated measurements (n = 10 for XRF and n = 4 for LOI measurements).
[$] Recommended, certified, or information value (https://gbank.gsj.jp/geostandards/welcome.html)
[$$] Note that the concentration is higher than the upper limit of calibration line (Table 6).
[¥] n.d.: not determined.
[¥¥] n.r. not reported.

Table 8. Detection limit of trace element.

calib. line*	2	4	5	6
n**	10	10	10	10
S (ppm)	4.9	7	—	—
V	2.1	1.1	0.9	2.3
Cr	1.5	1.7	2.0	5.8
Co	0.4	0.2	1.2	6.4
Ni	1.4	2.2	1.2	2.6
Cu	1.2	0.9	1.7	3.5
Zn	0.7	0.5	0.5	2.3
As	—	0.3	—	—
Rb	0.3	0.6	0.3	2.8
Sr	0.4	0.4	0.3	1.4
Y	0.5	0.5	0.4	2.3
Zr	0.3	0.5	0.3	1.6
Nb	0.3	0.3	0.2	0.7
Ba	4.1	3.1	3.1	17.2
Ce	2.5	3.2	2.8	—
Pb	0.7	0.4	0.6	—
Th	1.1	0.6	0.3	1.9

* Type of calibration line (see Table 4)
** Number of analyses.

two counters are not suitable values, then we conduct machine tuning and determine new calibration lines. To check the X-ray intensity fluctuation during measurement, reference samples (JB-1 for igneous and JSd-1 for sediment measurements) are analyzed every 15 to 20 samples. If measured compositions of the reference sample show fluctuation that exceed twice the standard deviation from the repeated analysis, then the analysis is suspended to check for analytical and machine condition error.

Table 8 lists the lower limits of detection (LLDs) of trace elements for four types of calibration lines that were calculated using the results of repeated analyses (10 times) of a blank sample (pure SiO_2; Cat. No. 37049-30, Kanto Chemical Co. Inc.). The LLDs are defined as three times the standard deviation of the analytical results (Tani *et al.*, 2005). For the three types of calibration lines with X-ray beam diameter of 30 mm (calibration types 2, 4 and 5), the LLDs for all elements are 0.2–2.1 ppm, except for Ba (up to 4.1 ppm) and Ce (up to 3.2 ppm). However, the LLDs for most elements using calibration type 6 (with the beam diameter of 10 mm) are more than 2 ppm (Table 8) due to the distinctly lower X-ray intensities resulting from the small beam diameter.

Analytical results of JB-1b, JA-1a and JSd-4

In order to further the estimate accuracy and precision of analytical results for unknown samples, three relatively new GSJ standard materials (JB-1b, JA-1a, and JSd-4) were measured (Table 7). GSJ has reported reference or certified values for the major elements of the three samples (Terashima *et al.*, 1998; GSL Geochemical Reference samples DataBase, AIST). Our analytical results are the same as the recommended (or certified) values within the accuracy of calibration lines for the major elements (Table 7).

Reference values are reported for several trace elements in JB-1b (Terashima *et al.*, 1998), but only information values are proposed for some trace elements in JA-1a and JSd-4 (GSL Geochemical Reference samples DataBase, AIST). Table 7 shows that most of our analytical values are in agreement with the reference (or information) values when we consider the accuracy of the calibration lines (Table 5). However, large differences are present between the analytical results and reference (or information) values for Cr in JB-1b, Cr, Cu, Zn, and Pb in JSd-4 (Table 7). The disagreement may indicate low accuracy of our analytical results or low reliability of the reference and information values for the trace elements.

Summary

(1) Routine sample preparation procedures suitable for XRF measurement and trace element analysis have been established.

(2) Quantitative analysis of 10 major elements (Si, Ti, Al, Fe, Mn, Mg, Ca, Na, K, P) in igneous rocks and sediments (that include ore and metamorphic rocks) have been established. The acquired data show good analytical accuracy and precision suitable for practical use in earth science discussions.

(3) Quantitative analysis of 17 trace elements (S, V, Cr, Co, Ni, Cu, Zn, As, Rb, Sr, Y, Zr, Nb, Ba, Ce, Pb, Th) in igneous rocks and sediments has been established. The analytical condition, and corrections for spectrum overlap and matrix effects are properly adjusted to acquire good analytical precision for measurements of igneous rocks and sediments.

Acknowledgements

This research was financially supported by Japan Society for the Promotion of Science (JSPS) KAKENHI Grant Number 18H05447 and the project of the National Museum of Nature and Science, Chemical Stratigraphy and Dating as a Clue for Understanding the History of the Earth and Life. We thank Ryo Amma for providing the JSPS budget, Keiko Matsui for analytical support, and Yukiyasu Tsutsumi for a peer review.

References

Czamanske, G. K., Hower, J. and Millard, R. C. (1966) Non-proportional, non-linear results from X-ray emission techniques involving moderate-dilution rock fusion. Geochemica et Cosmochimica Acta, **30**: 745–756.

Geological and Environmental Reference Materials (GeoRem). http://georem.mpch-mainz.gwdg.de/

Gladney, E. S. and Roelandts, I. (1987) 1987 compilation of elemental concentration data for USGS BIR-1, DNC-1 and W-2. *Geostandard Newsletter*, **12**: 63–118.

Gladney, E. S. and Roelandts, I. (1988) 1987 compilation of elemental concentration data for USGS BHVO-1, MAG-1, QLO-1, RGM-1, SCo-1, SDC-1, SGR-1 and STM-1. *Geostandard Newsletter*, **12**: 253–362.

Gladney, E. S. Jones, E. A., Nickell, E. J. and Roelandts, I. (1992) 1988 compilation of elemental concentration data for USGS AGV-1, GSP-1 and G-2. *Geostandard Newsletter*, **12**: 111–300.

GSL Geochemical Reference samples DataBase, AIST. https://gbank.gsj.jp/geostandards/welcome.html

Imai, N., Terashima, S., Itoh, S. and Ando, A. (1995) 1994 compilation of analytical data for minor and trace elements in seventeen GSJ geochemical reference samples, "igneous rock series". *Geostandard Newsletter*, **19**: 135–213.

Kimura, J. -I. and Yamada, Y. (1996) Evaluation of major and trace element XRF analyses using a flux to sample ratio of two to one glass beads. *Journal of Mineralogy, Petrology and Economic Geology*, **91**: 62–72.

Sano, T. (1995) Geology of Iki volcano group: Lava flow-stratigraphy mainly based on K-Ar dating. *Bulletin of the Volcanological Society of Japan*, **40**: 329–347. (in Japanese with English abstract)

Sano, T. (2002) Determination of major and trace element contents in igneous rocks by X-ray fluorescence spectrometer analysis. *Bulletin of Fuji Tokoha University*, **2**: 43–59. (in Japanese with English abstract)

Sano, T., Fukuoka, T. and Ishimoto, M. (2011) Petrological constraints on magma evolution of the Fuji volcano: A case study for the 1707 Hoei eruption, *Studies on the Origin and Biodiversity in the Sagami Sea Fossa Magna Element and the Izu–Ogasawara (Bonin) Arc*, *Memories of the National Museum of Nature and Science*, **47**: 471–496.

Sano, T., Shirao, M., Tani, K., Tsutsumi, Y., Kiyokawa, S. and Fujii, T. (2016) Progressive enrichment of arc magmas caused by the subduction of seamounts under Nishinoshima volcano, Izu–Bonin Arc, Japan. *Journal of Volcanology and Geothermal Research*, **319**: 52–65, doi: 10.1016/j.volgeores.2016.03.004.

Terashima, S. (1993) Three new GSJ rock reference samples: Rhyolite JR-2, Gabbro JGb-2 and Hornblendite JH-1. *Geostandard Newsletter*, **17**: 1–4.

Terashima, S., Taniguchi, M., Mikoshiba, M. and Imai, N. (1998) Preparation of two new GSJ geochemical reference materials: Basalt JB-1b and coal fly ash JCFA-1. *Geostandard Newsletter*, **22**: 113–117.

Tani, K., Orihashi, Y. and Nakada, S. (2002) Major and trace components analysis of silicate rocks by X-ray fluorescence spectrometer using fused glass beads: Evaluation of analytical precision of three, six, eleven times dilution fused glass beads methods. *Technical Research Report*, *Earth Research Institute*, *the University of Tokyo*, **8**: 26–36.

Tani, K., Kawabata, H., Chang, Q., Sato, K and Tatsumi, Y (2005) Quantitative analyses of silicate rock major and trace elements by X-ray fluorescence spectrometer: Evaluation of analytical precision and sample preparation. *Frontier Research on Earth Evolution: IFREE report*, **2**: 1–8.

Yamasaki, T. (2014) XRF major element analyses of silicate rocks using 1:10 dilution ratio glass bead and a synthetically extended calibration curve method. *Bulletin of the Geological Survey of Japan*, **65**: 97–103.

Yoshida, H. and Takahashi, N. (1997) Chemical behavior of major and trace elemements in the Horoman mantle diapir, Hidaka belt, Hokkaido, Japan. *Journal of Mineralogy, Petrology and Economic Geology*, **92**: 391–409. (in Japanese with English abstract)